



# Oxygen Exchange at the Internal Surface of Amorphous SiO<sub>2</sub> Studied by Photoluminescence of Isotopically Labeled Oxygen Molecules

著者	Kajihara Koichi, Miura Taisuke, Kamioka Hayato, Hirano Masahiro, Skuja Linards, Hosono Hideo
journal or publication title	Physical review letters
volume	102
number	17
page range	175502
year	2009-05
権利	(C) 2009 The American Physical Society
URL	<a href="http://hdl.handle.net/2241/102772">http://hdl.handle.net/2241/102772</a>

doi: 10.1103/PhysRevLett.102.175502

## Oxygen Exchange at the Internal Surface of Amorphous SiO<sub>2</sub> Studied by Photoluminescence of Isotopically Labeled Oxygen Molecules

Koichi Kajihara,<sup>1,2,\*</sup> Taisuke Miura,<sup>3</sup> Hayato Kamioka,<sup>4</sup> Masahiro Hirano,<sup>1,6</sup> Linards Skuja,<sup>1,5</sup> and Hideo Hosono<sup>1,6</sup>

<sup>1</sup>*Transparent Electro-Active Materials Project, ERATO-SORST, Japan Science and Technology Agency, in Frontier Research Center, S2-13, Tokyo Institute of Technology, 4259 Nagatsuta, Midori-ku, Yokohama 226-8503, Japan*

<sup>2</sup>*Department of Applied Chemistry, Graduate School of Urban Environmental Sciences, Tokyo Metropolitan University, 1-1 Minami-Osawa, Hachioji 192-0397, Japan*

<sup>3</sup>*Research & Development Division, OMRON Laserfront Inc., 1120 Shimokuzawa, Sagami-hara 229-1198, Japan*

<sup>4</sup>*Graduate School of Pure and Applied Sciences, University of Tsukuba, 1-1-1 Tennodai, Tsukuba 305-8571, Japan*

<sup>5</sup>*Institute of Solid State Physics, University of Latvia, Kengaraga iela 8, LV1063 Riga, Latvia*

<sup>6</sup>*Materials and Structures Laboratory & Frontier Research Center, Tokyo Institute of Technology, 4259 Nagatsuta, Midori-ku, Yokohama 226-8503, Japan*

(Received 12 February 2009; published 27 April 2009)

The exchange between lattice and interstitial oxygen species in an oxide was studied by the <sup>16</sup>O-<sup>18</sup>O isotope shift of the  $a^1\Delta_g(v=0) \rightarrow X^3\Sigma_g^-(v=1)$  infrared photoluminescence band of the oxygen molecules (O<sub>2</sub>) incorporated into the interstitial voids of amorphous SiO<sub>2</sub> (*a*-SiO<sub>2</sub>) by thermal annealing in <sup>18</sup>O<sub>2</sub> gas. A large site to site variation of the oxygen exchange rate, originating from structural disorder of *a*-SiO<sub>2</sub>, is found. The average exchange rate has an activation energy of ~2 eV, which is much larger than that for the diffusion of interstitial O<sub>2</sub> (~0.8–1.2 eV). The average exchange-free diffusion length of interstitial O<sub>2</sub> exceeds ~1 μm below 900 °C, providing definite evidence that oxygen diffuses as interstitial molecules in *a*-SiO<sub>2</sub>.

DOI: 10.1103/PhysRevLett.102.175502

PACS numbers: 61.72.jj, 65.60.+a, 66.30.hh, 78.55.Qr

Various properties of oxides relevant to practical applications, such as electrical and ionic conductivity, optical transparency, and catalytic activity, are closely related to the oxygen transfer between the oxides themselves and ambient oxygen molecules (O<sub>2</sub>). The interaction of O<sub>2</sub> with oxide surfaces has been studied extensively [1–3]. Amorphous SiO<sub>2</sub> (*a*-SiO<sub>2</sub>) is unique among oxides due to its low density and interstitial voids which may be treated as “internal surfaces.” The oxygen transfer occurring at the internal surfaces between the molecules in a “quasigas phase” and the surrounding lattice oxygen in the *a*-SiO<sub>2</sub> network is of fundamental interest because it is intrinsic, that is, unaffected by passivated dangling bonds and adatoms covering the outer surfaces. Moreover, the diffusion of interstitial O<sub>2</sub> in *a*-SiO<sub>2</sub> is technologically important as it is a key step in growing dielectric *a*-SiO<sub>2</sub> films on silicon microelectronic circuits [4,5]. It is considered that interstitial O<sub>2</sub> diffuses without significant exchange with the surrounding *a*-SiO<sub>2</sub> network [6–10]; however, some oxygen exchange has been found to occur [11–13]. The details have remained uncertain primarily because the concentration of interstitial O<sub>2</sub> is several orders of magnitude smaller than that of the background oxygen network atoms, and at the time of these studies, experimental techniques that are able to distinguish interstitial O<sub>2</sub> from the background were absent.

Oxygen molecules dissolved in solids and liquids can be selectively detected via their characteristic infrared (IR) photoluminescence (PL) due to the transition from the first singlet excited state  $a^1\Delta_g$  to the triplet ground state  $X^3\Sigma_g^-$

of O<sub>2</sub> (pure electronic band, PEB) [14,15]. This method has been useful in the study of the diffusion and reactions of O<sub>2</sub> in *a*-SiO<sub>2</sub> [16–18]. We demonstrate here that the oxygen exchange between interstitial O<sub>2</sub> and the *a*-SiO<sub>2</sub> network is quantitatively studied by combining the PL method with an isotope labeling technique. Since the shape and peak position of PEB are insensitive to isotopic substitution [19], the isotopologues of interstitial O<sub>2</sub> are distinguished using the PL band due to the transition from the *a* state to the first vibronic level of the *X* state  $X^3\Sigma_g^-(v=1)$  (vibrational sideband, VSB), which is much weaker than PEB but undergoes a strong isotope shift.

High-purity synthetic *a*-SiO<sub>2</sub> specimens (10 × 6.5 × 0.4–0.5 mm<sup>3</sup> with two optically polished faces) containing ~2 × 10<sup>18</sup> cm<sup>-3</sup> SiOH groups were sealed in an SiOH-free (SiOH ≤ 10<sup>17</sup> cm<sup>-3</sup>) silica tubes with <sup>18</sup>O<sub>2</sub> (<sup>18</sup>O isotopic purity ≥ 99%) or <sup>16</sup>O<sub>2</sub> gas of 0.9 atm at room temperature. The sealed silica tube, each containing eight specimens, were thermally annealed between 500 and 900 °C. Before and after the thermal annealing, the isotopic composition of O<sub>2</sub> gas in the silica tube was monitored by conventional Raman spectrometry [20] and was nearly unchanged [21]. The O<sub>2</sub>-loaded samples were taken out of the tube, and the PL bands were excited at 765 nm using an AlGaAs laser diode (~1.5 W at the sample position) via the forbidden transition to the second singlet excited state  $b^1\Sigma_g^+$  of interstitial O<sub>2</sub>. Since VSB is very weak, the eight specimens were stacked to facilitate the detection. The sample stack was irradiated normal to the polished face and the backscattered PL emission was re-

corded by a Fourier-transform IR Raman spectrometer (Model 960, Nicolet). The PL time decay curves were also measured (technique is described in Ref. [22]) to evaluate the possible variation in the PL quantum yield with the isotopic substitution.

Figure 1 shows PL spectra for samples thermally annealed in  $^{16}\text{O}_2$  or  $^{18}\text{O}_2$ . The  $^{16}\text{O}_2$  loading was performed for 72 h at 700 °C, whereas the  $^{18}\text{O}_2$  loading was done with a shorter time at lower temperature (12 h at 500 °C) to maximize  $^{18}\text{O}$  fraction in interstitial  $\text{O}_2$ . The spectra were normalized to the intensity of PEB at  $\sim 7855\text{ cm}^{-1}$  [15,23], showing a negligible shift upon  $^{18}\text{O}$  substitution. VSB of interstitial  $^{16}\text{O}_2$  PL was observed at  $\nu_{66} \approx 6308\text{ cm}^{-1}$ , and the band shape was simulated well with a pseudo Voigt function. In the  $^{18}\text{O}_2$ -loaded sample, VSB was shifted to a higher energy side along with a  $\sim 20\%$  increase in the normalized amplitude. This band is mainly due to interstitial  $^{18}\text{O}_2$  because the peak position agrees well with that expected from the atomic mass ratio between  $^{16}\text{O}$  and  $^{18}\text{O}$  and the PEB and VSB positions of interstitial  $^{16}\text{O}_2$  ( $\nu_{68} \approx 6352\text{ cm}^{-1}$  for  $^{16}\text{O}^{18}\text{O}$  and  $\nu_{88} \approx 6397\text{ cm}^{-1}$  for  $^{18}\text{O}_2$ ). However, its shape was slightly asymmetric due to small amounts of  $^{16}\text{O}^{18}\text{O}$  and  $^{16}\text{O}_2$  formed by oxygen exchange with the  $\alpha\text{-SiO}_2$  network. The observed spectrum was decomposed into three VSBs of  $^{16}\text{O}_2$ ,  $^{16}\text{O}^{18}\text{O}$ , and  $^{18}\text{O}_2$  to evaluate the respective isotopic fractions  $f_{66}$ ,  $f_{68}$ , and  $f_{88}$  ( $f_{66} + f_{68} + f_{88} = 1$ ) as follows. The peak positions of VSBs were fixed at  $\nu_{66}$ ,  $\nu_{68}$ , and  $\nu_{88}$ . The peak amplitude and width of  $^{18}\text{O}_2$  VSB as well as  $f_{66}$  and  $f_{88}$  were treated as variables. The peak amplitude and width of  $^{16}\text{O}^{18}\text{O}$  VSB were assumed to be given by linear interpolations of those of  $^{16}\text{O}_2$  and  $^{18}\text{O}_2$  VSBs. This procedure confirmed the high  $^{18}\text{O}$  purity ( $f_{88} + f_{68}/2 \sim 0.97$ ) of  $\text{O}_2$  in the  $^{18}\text{O}_2$ -loaded sample and determined the peak pa-

rameters of VSBs of interstitial  $^{18}\text{O}_2$  and  $^{16}\text{O}^{18}\text{O}$  that are needed for the following concentration analysis based on VSBs.

Figure 2 shows the VSB spectra for the samples thermally annealed at 700 °C in  $^{16}\text{O}_2$  or  $^{18}\text{O}_2$  for up to 72 h. The spectra of the  $^{18}\text{O}_2$ -loaded samples clearly consisted of three VSBs of interstitial  $^{16}\text{O}_2$ ,  $^{16}\text{O}^{18}\text{O}$ , and  $^{18}\text{O}_2$ . The  $^{18}\text{O}$  fraction of interstitial  $\text{O}_2$  ( $f_{88} + f_{68}/2$ ) decreased monotonically with an increase in annealing time, confirming the transfer of  $^{16}\text{O}$  from the  $\alpha\text{-SiO}_2$  network to interstitial  $\text{O}_2$ . Figure 3 summarizes variation of  $f_{66}$  and  $f_{88}$  with time and temperature of  $^{18}\text{O}_2$  loading.  $f_{66}$  and  $f_{88}$  evaluated by peak decomposition of the VSB spectra are denoted as filled symbols.

The total concentration of interstitial  $\text{O}_2$ ,  $C_T$ , was determined by comparing the PEB intensity with that of a reference sample of known interstitial  $^{16}\text{O}_2$  concentration [18]. The PL quantum yield of PEB is proportional to the decay constant  $\tau$  [22], and  $\tau_{68}$  and  $\tau_{88}$  were found to be  $\sim 1.7$  and  $\sim 2.5$  times larger than  $\tau_{66}$ , respectively. This uneven PL quantum yield was corrected by multiplying the PEB intensity with the factor  $\tau_{66}/(f_{66}\tau_{66} + f_{68}\tau_{68} + f_{88}\tau_{88})$ . The  $\text{O}_2$  concentrations evaluated with this procedure agree with those calculated from the Arrhenius relations of the solubility  $S$  and diffusion coefficient  $D$  determined from measurements above 800 °C [17,18]. Thus, the Arrhenius relations were used to produce  $D$ ,  $S$ , and  $C_T$  values in the following numerical simulation of the oxygen exchange.

The exchange of an interstitial  $\text{O}_2$  molecule with the  $\alpha\text{-SiO}_2$  network may be a reversible second order reaction, transferring only an oxygen atom in each exchange event [11,24],

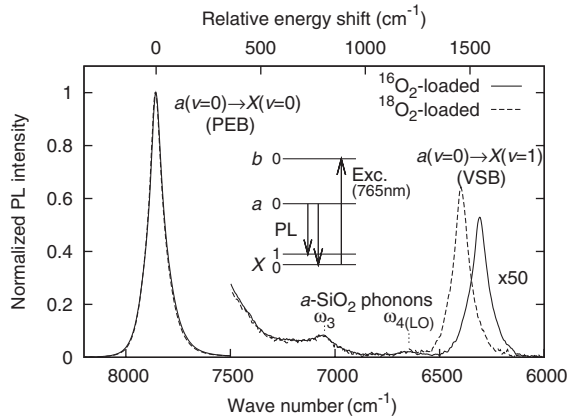
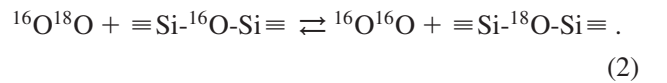
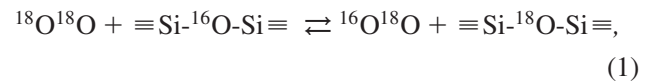


FIG. 1. PL spectra of interstitial  $\text{O}_2$  in samples thermally annealed in  $^{16}\text{O}_2$  for 72 h at 700 °C or  $^{18}\text{O}_2$  for 12 h at 500 °C. Schematic diagram of interstitial  $\text{O}_2$  energy levels is also shown. The spectra were normalized to the amplitude of the pure electronic band (PEB) at  $\sim 7855\text{ cm}^{-1}$ . The vibrational sideband (VSB) appears at  $\sim 6300\text{--}6400\text{ cm}^{-1}$ . Small peaks located between  $6500\text{--}7500\text{ cm}^{-1}$  are due to interactions with phonons of the  $\alpha\text{-SiO}_2$  network.

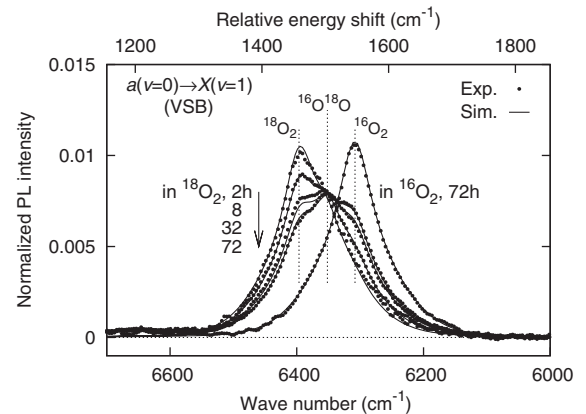


FIG. 2. Experimental and simulated VSB spectra normalized to the PEB amplitude for samples thermally annealed at 700 °C in  $^{16}\text{O}_2$  or  $^{18}\text{O}_2$ .

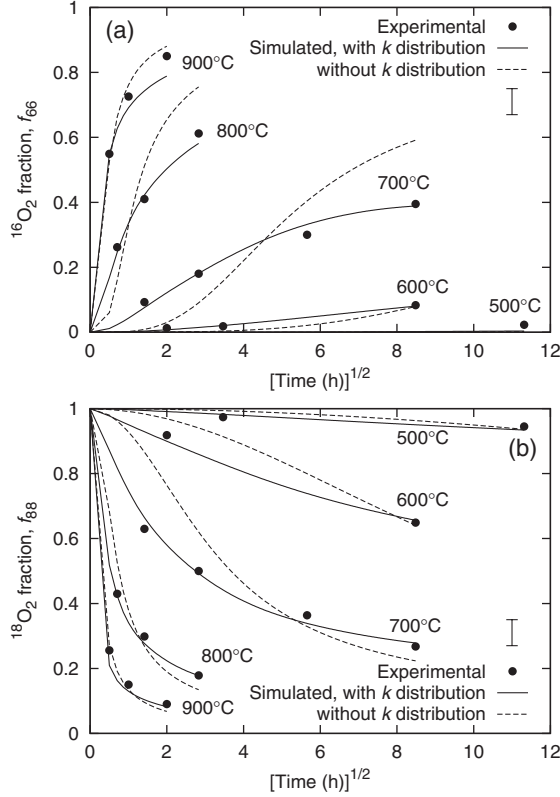


FIG. 3. Variation of the fractions of (a) interstitial  $^{16}\text{O}_2$  and (b)  $^{18}\text{O}_2$  ( $f_{66}$  and  $f_{88}$ , respectively) with time and temperature of the thermal annealing in  $^{18}\text{O}_2$  gas. The filled symbols were derived by peak decomposition of VSB under the restriction condition  $f_{66} + f_{68} + f_{88} = 1$ . The solid and dashed lines were drawn by directly simulating the VSB spectra from the solutions of the rate equations Eq. (3)–(6). The simulation was performed both with and without considering the distribution in the exchange rate constant  $k$ . The error bars represent the experimental uncertainties.

We defined the exchange rate constant of Eq. (1) forward and Eq. (2) backward reactions as  $k$ . Then the rate constant of the Eq. (1) backward and Eq. (2) forward reactions apparently becomes  $k/2$  as only one oxygen atom in  $^{16}\text{O}^{18}\text{O}$  contributes to these reactions.  $k$  may be affected by the local configuration of the glass network, which differs from site to site due to the variation in the Si-O-Si angle and the local network topology [25,26]. We assumed that the network oxygen atoms have nonequal exchange rates  $k$  with a Gaussian probability distribution against  $\log k$  [27], and each  $k$  has an Arrhenius-type dependence on the absolute annealing temperature  $T$  with common preexponential rate constant. This distribution was approximated by a finite number  $i$  of components [28], each having exchange rate  $k_i$ . The concentrations of the network  $^{16}\text{O}$  and  $^{18}\text{O}$  atoms for the component  $i$  ( $N_i$  and  $N_i^*$ ) were normalized by the total concentration as  $N^T = \sum_i (N_i + N_i^*) = 4.41 \times 10^{22} \text{ cm}^{-3}$  [29]. The temporal and spatial variations of interstitial  $^{16}\text{O}_2$ ,  $^{16}\text{O}^{18}\text{O}$ , and  $^{18}\text{O}_2$  concentrations ( $C$ ,  $C^*$ , and  $C^{**}$  where  $C^T = C + C^* +$

$C^{**}$ ) were calculated by numerically solving following simultaneous one-dimensional diffusion-exchange equations.

$$\frac{\partial C^T}{\partial t} = D \frac{\partial^2 C^T}{\partial x^2}, \quad (3)$$

$$\frac{\partial C}{\partial t} = D \frac{\partial^2 C}{\partial x^2} + \sum_i k_i \left( \frac{C^*}{2} N_i - C N_i^* \right), \quad (4)$$

$$\frac{\partial C^{**}}{\partial t} = D \frac{\partial^2 C^{**}}{\partial x^2} + \sum_i k_i \left( -C^{**} N_i + \frac{C^*}{2} N_i^* \right), \quad (5)$$

$$\frac{\partial N_i^*}{\partial t} = -\frac{\partial N_i}{\partial t} = k_i \left( \frac{C^*}{2} N_i + C^{**} N_i - C N_i^* - \frac{C^*}{2} N_i^* \right). \quad (6)$$

VSB spectra (Fig. 2, solid lines) were calculated from the solutions and fitted to the observed spectra. A boundary condition was set as  $C^T = C^{**} = 0.9ST/298$  at the sample surfaces, taking into account that (i) solubility of  $\text{O}_2$  depends linearly on the  $\text{O}_2$  pressure inside the silica tube [17,30], which is roughly proportional to  $T$ , (ii) dissolution of  $\text{O}_2$  is much faster than the subsequent diffusion of interstitial  $\text{O}_2$  [16,17], and (iii) the  $^{18}\text{O}$  fraction of  $\text{O}_2$  gas in the tube remained close to 1 during the thermal annealing.

As shown in Fig. 3, the solutions of the rate equations Eqs. (3)–(6) (solid lines) agreed well with the experimental variation of  $f_{66}$  and  $f_{88}$  (filled symbols) when  $k$  is distributed; it was not possible to obtain a good fit using a single  $k$  value. The full width at half maximum of the distribution of  $\log k$  was  $\sim 9.7$  at  $500^\circ\text{C}$  and  $\sim 6.4$  at  $900^\circ\text{C}$ , indicating that a part of network oxygen atoms are much more reactive than the remaining network oxygen atoms. These more reactive sites easily release  $^{16}\text{O}$  and enhance the formation of interstitial  $^{16}\text{O}^{18}\text{O}$  and  $^{16}\text{O}_2$  in an early stage of the oxygen loading. Later in the reaction, however, such sites have been occupied by  $^{18}\text{O}$  while the remaining sites release  $^{16}\text{O}$  more gradually, slowing the increase in  $f_{66}$  and  $f_{68}$ .

The average exchange rate constant  $k_a$  for systems with a  $k$  distribution may be represented by the simple weighted average of  $k_i$  as  $k_a = \sum_i k_i (N_i + N_i^*) / N^T$ . Figure 4 shows the dependence of  $k_a$  on  $T$ , where  $k_a$  ranged from  $\sim 10^{-28}$  to  $\sim 10^{-23} \text{ cm}^3 \text{ s}^{-1}$  according to the change in  $T$  between 500 and  $900^\circ\text{C}$ . The activation energy for  $k_a$ , which may be given by assuming a linear relation between  $\log k_a$  and  $T^{-1}$ , was  $\sim 2.1 \text{ eV}$ . Secondary ion mass spectroscopy profiling studies have reported similar values ( $\sim 2.6$  [12] and  $\sim 1.7 \text{ eV}$  [13]), although they assumed first-order exchange reactions. These values are larger than the activation energy for the permeation of interstitial  $\text{O}_2$  in  $\alpha\text{-SiO}_2$  ( $\sim 0.8\text{--}1.2 \text{ eV}$  [17,30,31]), suggesting that the oxygen exchange is not the bottleneck for the permeation. In contrast, they are much smaller than the energies of the O-O bond in  $\text{O}_2$  ( $\sim 5.1 \text{ eV}$ ), and Si-O bond ( $\sim 4.7 \text{ eV}$ ), and the



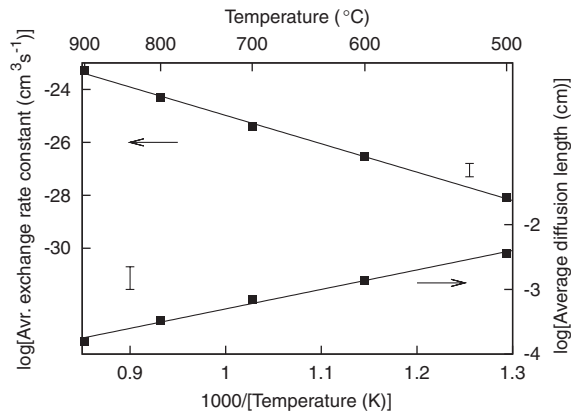


FIG. 4. Temperature dependence of the average exchange rate constant  $k_a$  and the average exchange-free diffusion length  $l$  of an interstitial  $O_2$  molecule [Eq. (7)]. The error bars represent the experimental uncertainties.

activation energy for the viscous flow of  $\alpha$ - $SiO_2$  ( $\sim 5$ – $7$  eV [32–34]) that is required for network rearrangement. Thus, the observed activation energy may correspond to the energy needed to form an activation complex during the oxygen exchange.

The average time interval of the oxygen exchange for an interstitial  $O_2$  molecule may be given by  $(k_a N^T)^{-1}$ , yielding  $\sim 3 \times 10^5$  s at  $500^\circ\text{C}$  and  $\sim 6$  s at  $900^\circ\text{C}$ . Using this value, the average exchange-free diffusion length  $l$  of an interstitial  $O_2$  molecule in one dimension may be calculated by

$$l = 2\left(\frac{D\tau}{\pi}\right)^{1/2} = 2\left(\frac{D}{\pi k_a N^T}\right)^{1/2}. \quad (7)$$

Calculated  $l$  values are plotted in Fig. 4; they were  $\sim 40$   $\mu\text{m}$  at  $500^\circ\text{C}$  and  $\sim 2$   $\mu\text{m}$  at  $900^\circ\text{C}$ , demonstrating that  $l$  is far larger than the scale of the ring and cage structures of the  $\alpha$ - $SiO_2$  network ( $\sim 1$  nm [26,29]).

In summary, we developed a photoluminescence technique to quantitatively study  $^{18}\text{O}$ -labeled interstitial  $O_2$  in amorphous  $SiO_2$ , which offers a direct way to investigate their property and intrinsic reactivity. The obtained results provide insight into interactions of  $O_2$  with oxides.

\*Author to whom correspondence should be addressed:  
kkaji@tmu.ac.jp

- [1] J. H. Lunsford, *Catal. Rev.* **8**, 135 (1974).
- [2] A. Bielański and J. Haber, *Catal. Rev.* **19**, 1 (1979).
- [3] M. Che and A. J. Tench, *Adv. Catal.* **32**, 1 (1983).
- [4] H. C. Lu, T. Gustafsson, E. P. Gusev, and E. Garfunkel, *Appl. Phys. Lett.* **67**, 1742 (1995).
- [5] M. L. Green, E. P. Gusev, and E. L. Garfunkel, *J. Appl. Phys.* **90**, 2057 (2001).
- [6] R. Rosencher, A. Straboni, S. Rigo, and G. Amsel, *Appl. Phys. Lett.* **34**, 254 (1979).

- [7] M. A. Lamkin, F. L. Riley, and R. J. Fordham, *J. Eur. Ceram. Soc.* **10**, 347 (1992).
- [8] A. Bongiorno and A. Pasquarello, *Phys. Rev. Lett.* **88**, 125901 (2002).
- [9] R. H. Doremus, *J. Non-Cryst. Solids* **349**, 242 (2004).
- [10] K. Tatsumura, T. Shimura, E. Mishima, K. Kawamura, D. Yamasaki, H. Yamamoto, T. Watanabe, M. Umeno, and I. Ohdomari, *Phys. Rev. B* **72**, 045205 (2005).
- [11] A. G. Revesz, B. J. Mrstik, and H. L. Hughes, *J. Electrochem. Soc.* **134**, 2911 (1987).
- [12] J. D. Cawley and R. S. Boyce, *Philos. Mag. A* **58**, 589 (1988).
- [13] J. D. Kalen, R. S. Boyce, and J. D. Cawley, *J. Am. Ceram. Soc.* **74**, 203 (1991).
- [14] C. Schweitzer and R. Schmidt, *Chem. Rev.* **103**, 1685 (2003).
- [15] L. Skuja, B. Güttler, D. Schiel, and A. R. Silin, *Phys. Rev. B* **58**, 14296 (1998).
- [16] K. Kajihara, T. Miura, H. Kamioka, M. Hirano, L. Skuja, and H. Hosono, *J. Ceram. Soc. Jpn.* **112**, 559 (2004).
- [17] K. Kajihara, H. Kamioka, M. Hirano, T. Miura, L. Skuja, and H. Hosono, *J. Appl. Phys.* **98**, 013529 (2005).
- [18] K. Kajihara, T. Miura, H. Kamioka, A. Aiba, M. Uramoto, Y. Morimoto, M. Hirano, L. Skuja, and H. Hosono, *J. Non-Cryst. Solids* **354**, 224 (2008).
- [19] R. Schmidt and E. Afshari, *Ber. Bunsen-Ges. Phys. Chem.* **96**, 788 (1992).
- [20] K. Kajihara, S. Matsuishi, K. Hayashi, M. Hirano, and H. Hosono, *J. Phys. Chem. C* **111**, 14855 (2007).
- [21]  $^{18}\text{O}$  fractions recorded before and after thermal annealing were  $\geq 0.99$  and  $\geq 0.97$ , respectively.
- [22] K. Kajihara, H. Kamioka, M. Hirano, T. Miura, L. Skuja, and H. Hosono, *J. Appl. Phys.* **98**, 013528 (2005).
- [23] Peak position determined by fitting with a pseudo Voigt function. The maximum is located at a bit higher energy,  $\sim 7857$   $\text{cm}^{-1}$ .
- [24] R. H. Doremus, *J. Electrochem. Soc.* **143**, 1992 (1996).
- [25] R. L. Mozzi and B. E. Warren, *J. Appl. Crystallogr.* **2**, 164 (1969).
- [26] *Defects in  $SiO_2$  and Related Dielectrics: Science and Technology*, edited by G. Pacchioni, L. Skuja, and D. L. Griscom, NATO Science Series II: Mathematics, Physics and Chemistry (Kluwer Academic Publishers, Dordrecht, Netherlands, 2000).
- [27] It corresponds to the Gaussian distribution in the activation energy for  $k$  when  $k$  follows an Arrhenius-type temperature dependence.
- [28] We set  $|i| \leq 15$  and confirmed that further increase in  $|i|$  does not influence the results.
- [29] R. H. Doremus, *Diffusion of Reactive Molecules in Solids and Melts* (John Wiley & Sons, New York, 2002).
- [30] F. J. Norton, *Nature (London)* **191**, 701 (1961).
- [31] C. C. Tournour and J. E. Shelby, *Phys. Chem. Glasses* **46**, 559 (2005).
- [32] G. Hetherington, K. H. Jack, and J. C. Kennedy, *Phys. Chem. Glasses* **5**, 130 (1964).
- [33] R. H. Doremus, *J. Appl. Phys.* **92**, 7619 (2002).
- [34] H. Kakiuchida, K. Saito, and A. J. Ikushima, *J. Appl. Phys.* **93**, 777 (2003).